

Extreme dimensional compression with quantum modelling

Thomas J. Elliott^{§,1,2,*} Chengran Yang^{§,2,1,†} Felix C. Binder^{2,1}

Andrew J. P. Garner^{3,4} Jayne Thompson⁴ and Mile Gu^{2,1,4,‡}

¹Complexity Institute, Nanyang Technological University, Singapore 637335

²School of Physical and Mathematical Sciences, Nanyang Technological University, Singapore 637371

³Institute for Quantum Optics and Quantum Information,

Austrian Academy of Sciences, Boltzmannngasse 3, Vienna 1090, Austria

⁴Centre for Quantum Technologies, National University of Singapore, 3 Science Drive 2, Singapore 117543

(Dated: May 25, 2022)

Effective and efficient forecasting relies on identification of the relevant information contained in past observations – the predictive features – and isolating it from the rest. When the future of a process bears a strong dependence on its behaviour far into the past, there are many such features to store, necessitating complex models with extensive memories. Here, we highlight a family of stochastic processes whose minimal classical models must devote unboundedly many bits to tracking the past. For this family, we identify quantum models of equal accuracy that can store all relevant information within a single two-dimensional quantum system (qubit). This represents the ultimate limit of quantum compression and highlights an immense practical advantage of quantum technologies for the forecasting and simulation of complex systems.

Predicting the future based on past events is a cornerstone of life. From meteorologists forecasting the weather, through investors trading on stock markets, to a predator chasing its prey, the ability to identify causes and accurately anticipate effects is central to survival and success. To carry out these essential tasks, models must be formulated, and information about past observations must be stored within memory.

In this context, processes with long historical dependence typically require models that store extensive information about past observations. This is because a model must ascribe each set of past causes that can give rise to distinct future effects to distinct configurations in its memory. When there are many such causes, the memory must support many configurations. Classically, the number of configurations is synonymous with the *dimension* of the memory – tracking a process with causes reaching far into the past typically requires a large memory with many dimensions.

In contrast, the number of configurations a quantum memory can take is separate from its dimension. This has led to quantum encodings with reduced memory dimension for several Markovian processes – where each output is conditional only on its immediate predecessor [1–4]. Here, we demonstrate that not only do these quantum advantages persist for non-Markovian processes, but that they become even more pronounced in this regime. We consider a family of such processes where the memory dimension required of a faithful classical model diverges with precision, and identify corresponding quantum models that compress all configurations into two dimensions.

This allows for all relevant history to be stored in a single two-state quantum system (*qubit*), evincing an extreme quantum advantage that scales without bound. Moreover, our protocol requires only a single probe qubit to extract the future statistics. This turns a problem from the converse scenario – that tracking a finite quantum system can require infinite classical resources [5–8] – into a useful tool.

This complements recent advances at the interface of complexity and quantum science, where it has been found that quantum models can drastically reduce the amount of past information – as measured by *information entropy* – that must be stored in memory to replicate the future behaviour of a process [1, 9–15]. Our work indicates that this advantage (along with its quantitative scaling divergences) also persists for the *memory dimension*. Crucially, this brings practical, verifiable, and significant quantum memory advantages within the reach of present technologies.

Framework and tools. A stochastic process \mathcal{X} can be characterised by an observation sequence $\overleftrightarrow{\mathcal{X}}$, detailing what happens and when [16]. We can partition this sequence in two: a past $\overleftarrow{\mathcal{X}}$ that describes everything that has happened up to the present; and a future $\overrightarrow{\mathcal{X}}$ describing everything yet to come (we use upper case to denote random variables, and lower case for their corresponding variates). The goal of causal modelling is to use the past (and only the past) to simulate the future [1, 17–19]. Specifically, a *causal model* \mathcal{M} stores in its memory states $m \in \mathcal{M}$ determined from an encoding function of the past $f : \{\overleftarrow{\mathcal{X}}\} \rightarrow \mathcal{M}$, such that it can produce futures $\overrightarrow{\mathcal{X}}$ according to $P(\overrightarrow{\mathcal{X}} | m = f(\overleftarrow{\mathcal{X}})) = P(\overrightarrow{\mathcal{X}} | \overleftarrow{\mathcal{X}})$.

Two widely-used metrics for a causal model’s memory efficiency are [17]:

- $C_{\mathcal{M}} := -\sum_{m \in \mathcal{M}} P(m) \log_2[P(m)];$
- $D_{\mathcal{M}} := \log_2[\dim(\mathcal{M})],$

*Electronic address: physics@tjelliott.net

†Electronic address: yangchengran92@gmail.com

‡Electronic address: mgu@quantumcomplexity.org

§These authors contributed equally to the results.

where $P(m) = \sum_{\overleftarrow{x} \in m} P(\overleftarrow{x})$ is the probability of finding the memory in state m in the process' steady-state. These measures respectively characterise the information stored by the memory and the dimension of the substrate into which it is encoded. Operationally, they represent the memory required to implement the model in an asymptotic ensemble (C_M) or single-shot (D_M) setting.

When \overleftarrow{X} is a bi-infinite, stationary sequence with discrete events, the ε -machine of computational mechanics [17–19] is the provably most efficient classical causal model according to both these metrics. The corresponding minimal measures are labelled as C_μ and D_μ , and referred to as the *statistical* and *topological complexity* respectively [17]. The key elements of these models are *causal states* $s \in \mathcal{S}$, a set of equivalence classes defined such that if two pasts have identical future predictions, the (causal state) memory encoding function $f_\varepsilon : \{\overleftarrow{x}\} \rightarrow \mathcal{S}$ assigns them to the same state: $f_\varepsilon(\overleftarrow{x}) = f_\varepsilon(\overleftarrow{x}') \Leftrightarrow P(\overrightarrow{X}|\overleftarrow{x}) = P(\overrightarrow{X}|\overleftarrow{x}')$. Causal states are in essence a state of knowledge, minimally encapsulating all information relevant to future prediction that can be obtained from observations of the past; they closely mirror the belief states of reinforcement learning [20, 21]. The ε -machine describes a stochastic transition structure between causal states, with transitions accompanied by the output of a symbol. This can be represented by a hidden Markov model [18]. These complexity measures have been applied to study structure in systems from a variety of fields, including neuroscience [22, 23], biology [24, 25], economics [26], geophysics [27], meteorology [28], and condensed matter physics [29].

These optimality results do not hold within the quantum domain [9]. For quantum causal models [1–4, 9–15, 30–37], each past \overleftarrow{x} is assigned a quantum state $|f(\overleftarrow{x})\rangle$ to be stored in the model memory. The efficiency metrics become $C_q := -\text{Tr}[\rho \log_2(\rho)]$ and $D_q := \log_2[\text{Tr}(\rho^0)]$, where $\rho = \sum_{\overleftarrow{x}} P(\overleftarrow{x}) |f(\overleftarrow{x})\rangle \langle f(\overleftarrow{x})|$. We refer to these as the *quantum statistical memory* and *quantum topological memory* of a model respectively; they inherit the same operational significance in the quantum regime as the corresponding classical quantities [9]. As with classical causal models, these quantum memory states encode information from the past of the process, and must not contain any information that can only be obtained from its future; the full description of a quantum model then includes the means by which its memory is probed to produce a sample of the future statistics given the observed past, which must similarly be drawn from $P(\overrightarrow{X}|m = |f(\overleftarrow{x})\rangle) = P(\overrightarrow{X}|\overleftarrow{x})$.

Current state-of-the-art constructions for quantum causal models [3] assign memory states directly from causal states $s \rightarrow |s\rangle$, though the optimal quantum encoding strategy is presently unknown for general processes [1, 34] – we therefore do not designate these quantum metrics as complexity measures. Nevertheless, it has been shown that in general there exists a quantum model with $C_q \leq C_\mu$ [9]. This quantum advan-

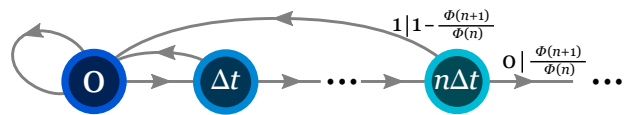


FIG. 1: **Tracking dual Poisson processes.** Causal models of dual Poisson processes track the confidence in chosen emission rate based on the time since last emission; the number of possible states diverges with refinement of timesteps. Since all states have different causal future distributions they each correspond to different causal states – the model depicted is the ε -machine. The notation $x|T$ indicates that with probability T the marked transition occurs while symbol x is output.

tage exploits the possibility to store quantum information in non-orthogonal states [38], enabling efficient isolation of predictive features. It has recently been shown that quantum models can also exhibit $D_q < D_\mu$ [1–4].

Dual Poisson processes. Consider a system that undergoes a series of Poissonian decay events through one of two channels with rates γ_1 and γ_2 . After each event, the decay channel for the next emission is chosen randomly, with probability p or $\bar{p} = 1 - p$ respectively. The choice of channel is hidden internally in the system, such that an external observer can only see when the decay events occur. Specifically, we consider an observer operating on discrete timesteps Δt , recording a 1 when an event occurs, and 0 otherwise. We call the resultant stochastic process a dual Poisson process, and it manifests as a series of 1s separated by strings of 0s. Note that the probabilistic choice of channel occurs only after events (1s), and remains unchanged across non-events (0s). The probability that a contiguous string of 0s (bookended by 1s) is of at least length n is given by the so-called survival probability $\Phi(n)$:

$$\Phi(n) = p\Gamma_1^n + \bar{p}\Gamma_2^n, \quad (1)$$

where $\Gamma_j = \exp(-\gamma_j \Delta t)$. We shall now look at the scaling of the memory metrics of causal models for such processes as the temporal precision Δt is refined – making the process increasingly non-Markovian. With arbitrary $\Phi(n)$ this framework describes general renewal processes [39].

Optimal classical causal model. Since the observer is unaware of the choice of decay channel, the information they must track reflects their confidence in the chosen rate based on the time since last emission. That is, a causal model of a dual Poisson process must track the number of 0s (\overleftarrow{n}) since the last 1 in order to predict how many more 0s (\overrightarrow{n}) until the next 1 appears; the direction of the arrows signifies that this is information to be obtained either from the past, or in the future. The relevant conditional future distribution is given by

$$P(\overrightarrow{N} = \overrightarrow{n} | \overleftarrow{n}) = \frac{\Phi(\overleftarrow{n} + \overrightarrow{n}) - \Phi(\overleftarrow{n} + \overrightarrow{n} + 1)}{\Phi(\overleftarrow{n})}. \quad (2)$$

When $\gamma_1 \neq \gamma_2$ and $p \neq 0, 1$ this conditional distribution is different for every \overleftarrow{n} . We can thus treat \overleftarrow{n} as being

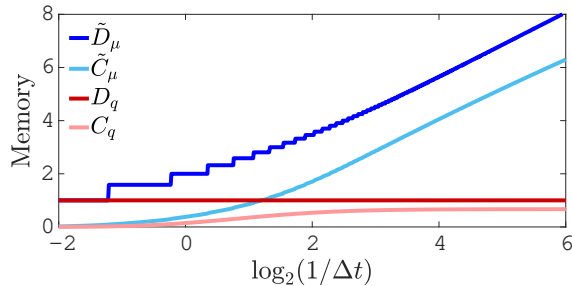


FIG. 2: **Scaling of memory metrics with precision.** Both classical memory metrics diverge with increasing precision, wherein the interval Δt is refined. In contrast, the quantum metrics remain finite, evincing an unbounded advantage: C_q tends to a bounded value, while D_q remains constant. Plot shown for $\gamma_1 = 12$, $\gamma_2 = 1$ and $p = 0.9$ (the qualitative features are typical for any non-extremal parameter choice).

synonymous with the causal states; the causal states are in effect counting the number of 0s since the last event. The ε -machine of the process is shown in Fig. 1.

From previous studies on the computational mechanics of renewal processes [40, 41], we can immediately identify that C_μ and D_μ are infinite in the continuum limit ($\Delta t \rightarrow 0$), as storing \overleftarrow{n} involves tracking an infinity of states with non-negligible occupation probabilities; we can understand this as arising from the increasing lengths of strings of 0s as timesteps are refined. Moreover, since $\Phi(\overleftarrow{n})$ remains non-zero for all \overleftarrow{n} , D_μ is also infinite at any level of discretisation. However, the differences between conditional probabilities become increasingly small for states at large $\overleftarrow{n} \Delta t$, and the probability of reaching such states is very small. We hence introduce a truncated form of the model, where after sufficiently large $\overleftarrow{n} \Delta t$ the causal states are all merged together (see Technical Appendix) – and study the associated complexities \tilde{C}_μ and \tilde{D}_μ of this model. Their scaling with increasing precision (i.e. decreasing Δt) for $\gamma_1 = 12$, $\gamma_2 = 1$ and $p = 0.9$ is shown in Fig. 2. Note that the qualitative features of this plot are typical for any non-extremal choice of parameters (i.e. $P \neq 0, 1$ and $\gamma_1 \neq \gamma_2$).

Unbounded quantum compression advantage.

We now show that this scaling divergence is a purely classical phenomenon, and need not persist in the quantum regime. By constructing quantum causal models of such processes for which the memory metrics are finite at any level of precision we show unbounded quantum advantages in compression, forming our main result.

Main Result: *A quantum causal model with $C_q \leq 1$ and $D_q \leq 1$ exists for any dual Poisson process at any level of precision Δt .*

Our models work by encoding the memory into one qubit, and using another to probe it [Fig. 3]. At each timestep, a constant unitary interaction U acts on both the memory and probe qubits, after which measurement (in the computational basis $\{|0\rangle, |1\rangle\}$) of the

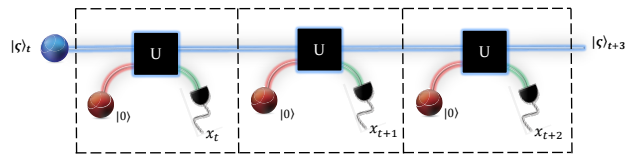


FIG. 3: **Two-qubit quantum model.** Our quantum models need only two qubits – one for the memory, and one to probe it. At each timestep a blank probe (red) is interacted with the memory qubit (blue) according to U , and subsequently measured (green). The measurement outcome forms the output of the process, and the memory automatically updates conditional on this outcome (the conditional dependence is not explicitly depicted here). The dashed boxes delineate the repeated fundamental building block of the model, representing each timestep.

probe qubit generates the corresponding output for the timestep [3, 14, 31]. We define a set of quantum memory states $\{|\zeta(n)\rangle\}$ corresponding to having observed n 0s since the last 1. We require

$$U|\zeta(n)\rangle|0\rangle = \sqrt{\frac{\Phi(n+1)}{\Phi(n)}}|\zeta(n+1)\rangle|0\rangle + \sqrt{1 - \frac{\Phi(n+1)}{\Phi(n)}}|\zeta(0)\rangle|1\rangle, \quad (3)$$

where the first subspace corresponds to the memory and the second the probe (reset to $|0\rangle$ at each timestep). To understand this criterion, consider the required action of U – for any quantum memory state $|\zeta(n)\rangle$ it must take the current memory state and blank probe state (left-hand side) to a state such that: (i) the measurement statistics of the probe in the computational basis are correct according to Eq. (2) (setting $\overleftarrow{n} = n$, with $\overleftarrow{n} = 0$ and the cumulative $\overleftarrow{n} > 0$ to obtain the probability for 1 and 0 respectively); and (ii) the quantum memory state is updated correctly according to this outcome ($|\zeta(n+1)\rangle$ for non-events 0, and reset to $|\zeta(0)\rangle$ for events 1). It can be seen that this is satisfied by the right-hand side of the condition, with the weightings corresponding to the probability (amplitudes) of the desired measurement statistics. Note that in principle we have the freedom to add a phase factor to the second term on the right-hand side; we do not include this here as it is not necessary for our construction.

In the Technical Appendix, we show that for any dual Poisson process the condition Eq. (3) is satisfied by the set of quantum memory states given by

$$|\zeta(n)\rangle = \frac{\sqrt{p\Gamma_1^n} + ig\sqrt{p\Gamma_2^n}}{\sqrt{\Phi(n)}}|0\rangle + \frac{i\sqrt{(1-g^2)p\Gamma_2^n}}{\sqrt{\Phi(n)}}|1\rangle, \quad (4)$$

where g is defined in the Technical Appendix, along with an explicit expression for U . Crucially, Eq. (4) evinces that the memory states can be encoded into a single

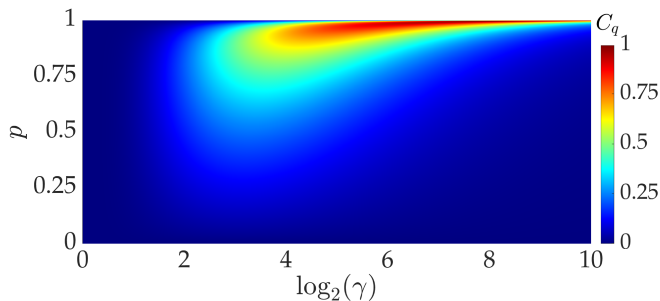


FIG. 4: **Quantum statistical memory of dual Poisson processes.** For much of the dual Poisson process family, the information stored by our quantum models is significantly less than one bit, highlighting that significant further compression is possible for ensemble simulators. The information stored is largest when both (i) the emission rates are significantly different, and (ii) the system is more likely to adopt the faster rate, as the state of confidence is frequently reset. $D_q = 1$ everywhere except the lines $P=0, 1$ and $\gamma=1$, where $D_q=0$.

qubit, guaranteeing $C_q \leq 1$ and $D_q \leq 1$. Moreover, since the process is generically not memoryless, and a binary system is the smallest possible memory, we can conclude that our model is (single-shot) minimal and that $D_q = 1$ is the quantum topological complexity. In Fig. 2 we compare the scaling of the quantum memory metrics with those of the minimal classical model. We thus observe the unbounded scaling of the quantum compression advantage in both ensemble and single-shot settings.

Finally, we calculate the quantum statistical memory C_q of our models in the continuum limit ($\Delta t \rightarrow 0$) for the whole dual Poisson process family. Due to the timescale invariance of C_q for renewal processes [14], the entire process family can be characterised by two parameters: $\gamma = \gamma_1/\gamma_2$ and p . Moreover, due to symmetries of the processes, $\{\gamma, p\}$ yields the same model as $\{\gamma^{-1}, \bar{p}\}$. In Fig. 4 we plot the continuum limit C_q for a broad parameter range. Interestingly, we see that for most choices of parameters $C_q \ll D_q$, suggesting yet further significant memory savings can be achieved in the ensemble regime. We see that C_q is largest when the two rates are significantly different (since the choice of decay channel has larger impact on the future) and the system predominantly picks the faster rate (since the confidence in the choice of channel is frequently reset).

Relationship to other works. We have shown that quantum dimensional advantages in causal modelling of classical stochastic processes can grow without bound. The highly cross-disciplinary nature of this work necessarily invites comparison with a range of prior and current research directions, and remarks on these relationships are in order. Foremost, a number of previous studies have shown unbounded quantum memory advantages in ensemble settings [12–15], where the advantage is contingent on an asymptotically-large set of simulators acting in parallel with a shared memory. A scaling advantage in terms of dimension has previously been

found for a Markovian process [1], albeit at the cost of an unboundedly-large alphabet (and hence output register). Thus, while theoretically demonstrating the scaling quantum memory advantages, these advantages are not presently experimentally feasible due to the need to either implement many simulators at once, or assign an ancilla of unbounded dimension for the output register. In contrast, our proposal requires only two qubits to demonstrate its advantage (and the associated scaling), and so is eminently more practical to implement; moreover, our proposal is the smallest possible that could ever demonstrate such an advantage, in the sense that if either the memory or output register of a model has fewer than two states then the process it simulates is trivial and/or memoryless.

The modelling of quantum dynamics with classical simulators is well-studied; several works approaching this problem from a variety of angles show that it typically requires unbounded classical resources to track the dynamics of a finite quantum system, due to the continuous nature of the Hilbert space it occupies [5–8]. Here, by reversing the scenario we show that this problem can turn into an asset – the very properties of (even simple) quantum systems that make them appear complex to classical systems can turn complex classical problems into simple quantum ones.

The use of complex amplitudes to define the memory state encodings has previously been considered for models with a small number of states, where it has been shown to offer reductions in both entropic and dimensional memory requirements relative to quantum models based on real amplitudes [3]. By using such phases to achieve compression of the memory into a single qubit we have addressed a conjecture made in this work regarding the potential of complex encodings to offer significant enhancements to the quantum advantage.

We note that despite a degeneracy in nomenclature, our framework is distinct from quantum causal models [42] in the sense of causal inference [43]. Yet, the overlap in terminology is understandable: in such works the goal is to identify causal relationships between variables, e.g., to determine one variable *causes* the value of another, or if both stem from a common cause; on the other hand we start from the proposition that the past causes the future, and seek to identify *what* the information in the past observations is that gives rise to (i.e., causes) the future statistics. Finally, we also note a resemblance between our discretised models using an ancillary system to interrogate a memory qubit and recent work on models of quantum clocks [44].

Concluding remarks. The single-shot setting of our advantage is ideal for current and near-future quantum technologies. Crucially, such dimensional advantages can be more readily verified than corresponding entropic advantages; one need only count the dimension of the memory system, rather than perform full tomography [4]. The small-scale quantum systems required for our proposal are highly amenable to present experimental ca-

pabilities; they could for instance be implemented with current two-qubit ion trap experiments, where sequential interaction-measurement-feedback cycles have been realised [45]. Indeed, consideration of resources in the experimentally more straightforward single-shot regime has garnered notable interest in other contexts [46–56].

While we have shown an unbounded dimensional scaling advantage for the dual Poisson process specifically, our findings motivate future work to investigate the typicality of processes that admit such single-shot advantages, particularly with the introduction of complex amplitudes, as well as approximate compression techniques for those that do not. Indeed, the behaviour of a broader range of renewal processes can be captured by generalising Eq. (4) to have different amplitudes and include additional states. A clear direction to extend these techniques for scaling advantages is to other continuous parameters such as spatial co-ordinates [12], or more abstract settings such as continuous belief spaces [20].

Interestingly, while both our quantum model and the optimal classical model provide an approximation of the fully-continuous process for finite timesteps Δt , in the quantum case a decrease in timestep size is not accompanied by an increase in memory size. The quantum model memory size D_q is entirely independent of the timestep, and does not exhibit the classical scaling of memory with precision. This indicates that the limiting factor in the accuracy of quantum models of such processes is not the available memory, but the accuracy with which it can be addressed. Our results already in some sense indicate a robustness of the quantum advantage: errors in the implementation of the quantum model can be accounted for by limiting the precision Δt to not exceed that achievable by the experiment – and the problem of noise exceeding the difference in future statistics for large \overleftarrow{n} is mitigated by the truncated process; Ultimately, while it would not be possible to witness the scaling difference all the way up to the continuum limit, it can still be shown up to the best achievable precision. We note that while errors present in current quantum technologies would not prevent us from demonstrating that our quantum models can achieve better precision than any classical model at a fixed number of (qu)bits, the possibility to address larger numbers of classical bits with smaller errors than qubits on quantum computers would presently allow classical computers to achieve a higher level of precision. Nevertheless, our results suggest compression tasks as a potential future route for demonstrating absolute superiority of quantum technologies over classical devices, and as a critical application of these incipient devices.

Technical Appendix

Truncated dual Poisson processes. As noted above, D_μ remains infinite at any level of discretisation, as there is no maximum \overleftarrow{n} that the processes cannot exceed, and no merging of different \overleftarrow{n} into the same causal

state. However, keeping this infinite overhead of states provides very little additional predictive power at large $\overleftarrow{n}\Delta t$, as the probability of the process reaching these states is small, and the difference in conditional probabilities between $\overleftarrow{n} = n$ and $\overleftarrow{n} = n + 1$ is monotonically decreasing towards zero with increasing n . We therefore introduce a truncated form of the process, where there is a designated ‘terminal’ state at n_{term} , such that all states at $\overleftarrow{n} = n > n_{\text{term}}$ are merged down into this state. This terminal state must have transition probabilities that are a weighted average of all the merged states; when an event happens the model transitions to $\overleftarrow{n} = 0$ as before, but now on non-events the system remains in the $n = n_{\text{term}}$ state, as opposed to advancing further.

There is a level of subjective choice in how n_{term} is selected. Appropriate methods can be for example based on the fidelity of the conditional distributions at larger \overleftarrow{n} , or on the probabilities of reaching such states. For concreteness, we pick a straightforward criterion:

$$n_{\text{term}} := \min_{n \in \mathbb{N}} n |\Phi(n) \leq \delta(1 - \Phi(1)). \quad (5)$$

That is, n_{term} is the first state for which the probability of reaching said state is less than a fraction δ of the probability of decay in the first timestep. We here use $\delta = 0.01$.

Quantum model construction. As described in the main text, a unitary U and set of quantum memory states $\{|\zeta(n)\rangle\}$ that satisfy Eq. (3) form a quantum causal model of the dual Poisson process at a particular set of parameters. Here we show that the memory states given by Eq. (4) form such a set of states, and give the corresponding U . This will prove our main result.

We begin by postulating a unitary operator U that is stipulated to act in the following manner on two (non-orthogonal) states $\{|\phi_1\rangle, |\phi_2\rangle\}$ that we refer to as ‘generator’ states:

$$U|\phi_j\rangle|0\rangle = \sqrt{\Gamma_j}|\phi_j\rangle|0\rangle + \sqrt{1 - \Gamma_j}|\phi_R\rangle|1\rangle, \quad (6)$$

with $j \in \{1, 2\}$, and we refer to $|\phi_R\rangle := \sqrt{p}|\phi_1\rangle + i\sqrt{p}|\phi_2\rangle$ as the ‘reset’ state. We define the overlap of the two generator states $g := \langle\phi_1|\phi_2\rangle$, noting that it depends on the size of the timesteps Δt . Without loss of generality, we can enforce that this quantity be both real and positive. Analogous to current systematic approaches for constructing quantum causal models [3, 31] we utilise the relation $\langle\phi_1|\phi_2\rangle = \langle\phi_1|\langle 0|U^\dagger U|\phi_2\rangle|0\rangle$, which arises from the properties of unitary operators. From this, we obtain

$$g = \frac{\sqrt{(1 - \Gamma_1)(1 - \Gamma_2)}}{1 - \sqrt{\Gamma_1\Gamma_2}}. \quad (7)$$

Armed with this, we can now express the generator states in the computational basis of a qubit $\{|0\rangle, |1\rangle\}$. Without loss of generality, we can assign

$$\begin{aligned} |\phi_1\rangle &= |0\rangle \\ |\phi_2\rangle &= g|0\rangle + \sqrt{1 - g^2}|1\rangle. \end{aligned} \quad (8)$$

We see that after emitting a 1, the memory always transitions to the reset state $|\phi_R\rangle$; it defines the $\overline{n} = 0$ state to which the memory returns after the occurrence of an event. This thus corresponds to the memory state $|\zeta(0)\rangle$. The remaining $|\zeta(n)\rangle$ can be obtained by applying the unitary to the reset state n times and post-selecting on the probe being measured as $|0\rangle$ after each application: $|\zeta(n)\rangle \propto (\Pi_0 U)^n |\phi_R\rangle |0\rangle$, where $\Pi_0 = |0\rangle\langle 0|$ is the projector onto the non-event subspace of the probe. Accounting for normalisation, we obtain

$$|\zeta(n)\rangle = \frac{\sqrt{p\Gamma_1^n}}{\sqrt{\Phi(n)}} |\phi_1\rangle + \frac{i\sqrt{\bar{p}\Gamma_2^n}}{\sqrt{\Phi(n)}} |\phi_2\rangle. \quad (9)$$

By inserting Eq. (8) into Eq. (9) we recover the the memory states as prescribed in Eq. (4). We can similarly express U in the computational basis using Eqs. (6) and (8):

$$\begin{aligned} U|0\rangle|0\rangle &= \sqrt{\Gamma_1}|0\rangle|0\rangle \\ &+ \sqrt{1-\Gamma_1}(\sqrt{\bar{p}} + i\sqrt{\bar{p}g})|0\rangle|1\rangle \\ &+ i\sqrt{1-\Gamma_1}\sqrt{\bar{p}}\sqrt{1-g^2}|1\rangle|1\rangle \end{aligned} \quad (10)$$

and

$$\begin{aligned} U|1\rangle|0\rangle &= \frac{(\sqrt{\Gamma_2} - \sqrt{\Gamma_1})g}{\sqrt{1-g^2}}|0\rangle|0\rangle \\ &+ \sqrt{\Gamma_2}|1\rangle|0\rangle \\ &+ \left(\sqrt{1-\Gamma_2} - \sqrt{1-\Gamma_1}g\right) \frac{\sqrt{\bar{p}} + i\sqrt{\bar{p}g}}{\sqrt{1-g^2}}|0\rangle|1\rangle \\ &+ i\left(\sqrt{1-\Gamma_2} - \sqrt{1-\Gamma_1}g\right) \sqrt{\bar{p}}|1\rangle|1\rangle. \end{aligned} \quad (11)$$

The remaining two columns describing the action $U|0\rangle|1\rangle$ and $U|1\rangle|1\rangle$ are not uniquely defined by the model, and remain a free choice provided the unitarity of U is upheld. We can also construct a pair of Kraus operators $\{E_0, E_1\}$ that describe the effective evolution of the memory conditional on the observed output and may be used to update the memory when tracking an external system that behaves according to the process. These operators are defined according to $E_j = \langle j|U|0\rangle$, where the states in this expression belong to the probe subspace [38]; they can be readily obtained from Eqs. (10) and (11).

Finally, we verify that this model produces the correct survival probability for the process Eq. (1). This is found from the probability of recovering a contiguous string of n 0s after starting from the reset state:

$$\begin{aligned} \Phi(n) &= \langle \phi_R | \langle 0 | (U^\dagger \Pi_0)^n (\Pi_0 U)^n | \phi_R \rangle | 0 \rangle \\ &= p\Gamma_1^n + \bar{p}\Gamma_2^n. \end{aligned} \quad (12)$$

Thus, our construction faithfully replicates the process, and may be used to track the dynamics of any dual Poisson process, at any level of discretisation, thus proving our main result. Notably, our quantum models are free

from the need to introduce a truncation at long times as was done in the classical case.

As would be expected, the quantum memory states Eq. (9) and U Eqs. (10) and (11) depend on the particular parameters defining the specific dual Poisson process to be modelled. Nevertheless, once initialised in a particular memory state $|\zeta(n)\rangle$ corresponding to our observed past (which, being a qubit state, can always be prepared with at most three rotations from $\{R_y, R_z\}$ – corresponding to rotations of a qubit around the y and z axis of the Bloch sphere [57]), the model operates by repeated applications of the same unitary U , each followed by measurement and reset of the ancilla to simulate the future statistics. Being a two-qubit unitary, U can always be synthesised by at most fifteen rotations from $\{R_y, R_z\}$ and three CNOT gates [57, 58], irrespective of the parameters.

Considering current state-of-the-art ion trap experiments with gate fidelities in excess of 99.9% for two qubit gates, and 99.99% for single qubit gates [59, 60], we can naively estimate their fidelity in implementing U as being at least 99.5% when multiplying the fidelity in implementing the elementary gates (i.e., $0.999^3 \times 0.9999^{15}$). This estimate is likely too pessimistic, as it neglects that some single qubit gates are applied in parallel to different qubits, and that the errors can act in opposing directions to partially cancel each other out. Nevertheless, we can use this as a back-of-the-envelope benchmark for implementability. Using the parameters of Fig. 2 ($\gamma_1 = 12, \gamma_2 = 1, p = 0.9$) with $\log_2(1/\Delta t) = 4$, from Eqs. (10) and (11) we obtain

$$U = \begin{pmatrix} 0.6873 & -0.1788 & \# & \# \\ 0 & 0.9692 & \# & \# \\ 0.6891 + 0.1230i & -0.1605 - 0.0287i & \# & \# \\ 0.1940i & -0.0452i & \# & \# \end{pmatrix}, \quad (13)$$

where $\#$ indicates a ‘free’ value to be chosen subject to the constraint that the columns form mutually orthogonal vectors. By inspection, we can see that any implementation of this with at least 99.5% fidelity must capture the salient features to a high degree of accuracy. At this value of Δt the quantum scaling advantage is already clearly visible, and so is practical to verify with current ion trap experiments.

Calculating statistical complexity and quantum statistical memory. Prior work on the computational mechanics of renewal processes [40] has established that the steady-state probabilities of the causal states are proportional to their survival probabilities. That is, $P(\overline{n}) = \mu\Phi(\overline{n})$, where $\mu^{-1} := \sum_{n=0}^{\infty} \Phi(n)$. For dual Poisson processes,

$$\mu = \frac{(1-\Gamma_1)(1-\Gamma_2)}{p(1-\Gamma_2) + \bar{p}(1-\Gamma_1)}. \quad (14)$$

Thus, we have that $C_\mu = -\sum_{n=0}^{\infty} P(n) \log_2[P(n)]$ and

$$\tilde{C}_\mu = -\sum_{n=0}^{n_{\text{term}}-1} P(n) \log_2[P(n)] - P(n_{\text{term}}) \log_2[P(n_{\text{term}})], \quad (15)$$

where $P(n_{\text{term}}) = \sum_{n=n_{\text{term}}}^{\infty} P(n)$. Further, using Eq. (4) with $\rho = \sum_{n=0}^{\infty} P(n) |\zeta(n)\rangle \langle \zeta(n)|$ we obtain

$$\rho = \mu \left(\begin{array}{cc} \frac{p}{1-\Gamma_1} + \frac{g^2 \bar{p}}{1-\Gamma_2} & \frac{g\sqrt{(1-g^2)\bar{p}}}{1-\Gamma_2} - \frac{i\sqrt{(1-g^2)p\bar{p}}}{1-\sqrt{\Gamma_1\Gamma_2}} \\ \frac{g\sqrt{(1-g^2)\bar{p}}}{1-\Gamma_2} + \frac{i\sqrt{(1-g^2)p\bar{p}}}{1-\sqrt{\Gamma_1\Gamma_2}} & \frac{(1-g^2)\bar{p}}{1-\Gamma_2} \end{array} \right), \quad (16)$$

which may be straightforwardly diagonalised to find the two eigenvalues $\{\lambda_1, \lambda_2\}$, and hence calculate $C_q = -\lambda_1 \log_2(\lambda_1) - \lambda_2 \log_2(\lambda_2)$.

Acknowledgements

This work was funded by the Lee Kuan Yew Endowment Fund (Postdoctoral Fellowship), grant FQXi-RFP-1809 from the Foundational Questions Institute and Fetzer Franklin Fund (a donor advised fund of Silicon Valley Community Foundation), Singapore Ministry of Education Tier 1 grant RG190/17, National Research Foundation Fellowship NRF-NRFF2016-02, and National Research Foundation and Agence Nationale de la Recherche joint Project No. NRF2017-NRFANR004 VanQuTe. T.J.E., C.Y., and F.C.B. thank the Centre for Quantum Technologies for their hospitality.

-
- [1] J. Thompson, A. J. P. Garner, J. R. Mahoney, J. P. Crutchfield, V. Vedral, and M. Gu, *Physical Review X* **8**, 031013 (2018).
- [2] S. Loomis and J. P. Crutchfield, arXiv:1808.08639 (2018).
- [3] Q. Liu, T. J. Elliott, F. C. Binder, C. Di Franco, and M. Gu, *Physical Review A* **99**, 062110 (2019).
- [4] F. Ghafari, N. Tischler, J. Thompson, M. Gu, L. K. Shalm, V. B. Verma, S. W. Nam, R. B. Patel, H. M. Wiseman, and G. J. Pryde, arXiv:1812.04251 (2018).
- [5] A. Monras and A. Winter, *Journal of Mathematical Physics* **57**, 015219 (2016).
- [6] A. Cabello, M. Gu, O. Gühne, J.-Å. Larsson, and K. Wiesner, *Physical Review A* **94**, 052127 (2016).
- [7] A. Cabello, M. Gu, O. Gühne, and Z.-P. Xu, *Physical Review Letters* **120**, 130401 (2018).
- [8] P. Warszawski and H. M. Wiseman, arXiv:1905.10935 (2019).
- [9] M. Gu, K. Wiesner, E. Rieper, and V. Vedral, *Nature Communications* **3**, 762 (2012).
- [10] J. R. Mahoney, C. Aghamohammadi, and J. P. Crutchfield, *Scientific Reports* **6**, 20495 (2016).
- [11] M. S. Palsson, M. Gu, J. Ho, H. M. Wiseman, and G. J. Pryde, *Science Advances* **3**, e1601302 (2017).
- [12] A. J. P. Garner, Q. Liu, J. Thompson, V. Vedral, et al., *New Journal of Physics* **19**, 103009 (2017).
- [13] C. Aghamohammadi, J. R. Mahoney, and J. P. Crutchfield, *Scientific Reports* **7** (2017).
- [14] T. J. Elliott and M. Gu, *npj Quantum Information* **4**, 18 (2018).
- [15] T. J. Elliott, A. J. P. Garner, and M. Gu, *New Journal of Physics* **21**, 013021 (2019).
- [16] A. Khintchine, *Mathematische Annalen* **109**, 604 (1934).
- [17] J. P. Crutchfield and K. Young, *Physical Review Letters* **63**, 105 (1989).
- [18] C. R. Shalizi and J. P. Crutchfield, *Journal of Statistical Physics* **104**, 817 (2001).
- [19] J. P. Crutchfield, *Nature Physics* **8**, 17 (2012).
- [20] A. R. Cassandra, L. P. Kaelbling, and M. L. Littman, in *Proceedings of the Twelfth AAAI National Conference on Artificial Intelligence* (AAAI Press, 1994), pp. 1023–1028.
- [21] L. P. Kaelbling, M. L. Littman, and A. W. Moore, *Journal of artificial intelligence research* **4**, 237 (1996).
- [22] R. Haslinger, K. L. Klinkner, and C. R. Shalizi, *Neural Computation* **22**, 121 (2010).
- [23] S. E. Marzen, M. R. DeWeese, and J. P. Crutchfield, *Frontiers in Computational Neuroscience* **9**, 105 (2015).
- [24] C.-B. Li, H. Yang, and T. Komatsuzaki, *Proceedings of the National Academy of Sciences* **105**, 536 (2008).
- [25] D. Kelly, M. Dillingham, A. Hudson, and K. Wiesner, *PloS one* **7**, e29703 (2012).
- [26] J. B. Park, J. W. Lee, J.-S. Yang, H.-H. Jo, and H.-T. Moon, *Physica A: Statistical Mechanics and its Applications* **379**, 179 (2007).
- [27] R. W. Clarke, M. P. Freeman, and N. W. Watkins, *Physical Review E* **67**, 016203 (2003).
- [28] A. J. Palmer, C. W. Fairall, and W. A. Brewer, *IEEE Transactions on Geoscience and Remote Sensing* **38**, 2056 (2000).
- [29] D. P. Varn, G. S. Canright, and J. P. Crutchfield, *Physical Review B* **66**, 174110 (2002).
- [30] F. Ghafari Jouneghani, M. Gu, J. Ho, J. Thompson, W. Y. Suen, H. M. Wiseman, and G. J. Pryde, arXiv:1711.03661 (2017).
- [31] F. C. Binder, J. Thompson, and M. Gu, *Physical Review Letters* **120**, 240502 (2018).
- [32] C. Aghamohammadi, J. R. Mahoney, and J. P. Crutchfield, *Physics Letters A* **381**, 1223 (2016).
- [33] P. M. Riechers, J. R. Mahoney, C. Aghamohammadi, and J. P. Crutchfield, *Physical Review A* **93**, 052317 (2016).
- [34] W. Y. Suen, J. Thompson, A. J. P. Garner, V. Vedral, and M. Gu, *Quantum* **1**, 25 (2017).
- [35] J. Thompson, A. J. P. Garner, V. Vedral, and M. Gu, *npj Quantum Information* **3**, 6 (2017).
- [36] C. Aghamohammadi, S. P. Loomis, J. R. Mahoney, and J. P. Crutchfield, *Physical Review X* **8**, 011025 (2018).
- [37] C. Yang, F. C. Binder, V. Narasimhachar, and M. Gu, *Physical Review Letters* **121**, 260602 (2018).
- [38] M. A. Nielsen and I. Chuang, *Quantum Computation and Quantum Information* (2000).
- [39] W. L. Smith, *Journal of the Royal Statistical Society. Series B (Methodological)* pp. 243–302 (1958).
- [40] S. E. Marzen and J. P. Crutchfield, *Entropy* **17**, 4891 (2015).

- [41] S. Marzen and J. P. Crutchfield, *Journal of Statistical Physics* **168**, 109 (2017).
- [42] J.-M. A. Allen, J. Barrett, D. C. Horsman, C. M. Lee, and R. W. Spekkens, *Physical Review X* **7**, 031021 (2017).
- [43] J. Pearl, *Causality: models, reasoning and inference*, vol. 29 (Springer, 2000).
- [44] M. P. Woods, R. Silva, G. Pütz, S. Stupar, and R. Renner, arXiv:1806.00491 (2018).
- [45] V. Negnevitsky, M. Marinelli, K. Mehta, H.-Y. Lo, C. Flühmann, and J. P. Home, *Nature* **563**, 527 (2018).
- [46] R. Renner, *International Journal of Quantum Information* **6**, 1 (2008).
- [47] L. Del Rio, J. Åberg, R. Renner, O. Dahlsten, and V. Vedral, *Nature* **474**, 61 (2011).
- [48] F. G. S. L. Brandao and N. Datta, *IEEE Transactions on Information Theory* **57**, 1754 (2011).
- [49] L. Wang and R. Renner, *Physical Review Letters* **108**, 200501 (2012).
- [50] M. Tomamichel and M. Hayashi, *IEEE Transactions on Information Theory* **59**, 7693 (2013).
- [51] J. Åberg, *Nature Communications* **4**, 1925 (2013).
- [52] M. Horodecki and J. Oppenheim, *Nature Communications* **4**, 2059 (2013).
- [53] N. Y. Halpern, A. J. P. Garner, O. C. O. Dahlsten, and V. Vedral, *New Journal of Physics* **17**, 095003 (2015).
- [54] M. Tomamichel, *Quantum Information Processing with Finite Resources: Mathematical Foundations*, vol. 5 (Springer, 2015).
- [55] K. Korzekwa, M. Lostaglio, J. Oppenheim, and D. Jennings, *New Journal of Physics* **18**, 023045 (2016).
- [56] B. Regula, K. Fang, X. Wang, and G. Adesso, *Physical Review Letters* **121**, 010401 (2018).
- [57] F. Vatan and C. Williams, *Physical Review A* **69**, 032315 (2004).
- [58] B. Kraus and J. I. Cirac, *Physical Review A* **63**, 062309 (2001).
- [59] T. P. Harty, D. T. C. Allcock, C. J. Ballance, L. Guidoni, H. A. Janacek, N. M. Linke, D. N. Stacey, and D. M. Lucas, *Physical Review Letters* **113**, 220501 (2014).
- [60] C. J. Ballance, T. P. Harty, N. M. Linke, M. A. Sepiol, and D. M. Lucas, *Physical Review Letters* **117**, 060504 (2016).